Contribution from the Kenan Laboratories of Chemistry,
The University of North Carolina, Chapel Hill, North Carolina 27514

Electrochemical Polymerization of Amino-, Pyrrole-, and Hydroxy-Substituted Tetraphenylporphyrins

A. Bettelheim,† B. A. White, S. A. Raybuck,‡ and Royce W. Murray*

Received July 30, 1986

The electrochemical polymerizations of tetrakis(*o*-, *m*-, and *p*-aminophenyl)porphyrin, tetrakis(*p*-(dimethylamino)phenyl)porphyrin, tetrakis(*p*-hydroxyphenyl)porphyrin, and tetrakis(*p*-*N*-pyrrolylphenyl)porphyrin and their nickel and cobalt metalated complexes are described. Oxidations of these monomers lead to thin polymeric coatings on electrodes by coupling reactions analogous to those operative in polyaniline, polypyrrole, and polyphenol electropolymerization. The films contain from two to several hundred layers of porphyrin sites and display reductive electrochemical and electronic spectroscopic properties similar to those of monomer solutions in acetonitrile or methylene chloride. The pyrrolyl- and amino-based polymers are polycationic and thus anion exchangers, whereas the hydroxy-based polymers (at pH >8) are polyanionic. Films prepared from electropolymerization of cobalt tetrakis(*o*-aminophenyl)porphyrin display a split Co(III/II) wave in aqueous acid and base and are good oxygen reduction catalysts, whereas films prepared from all other cobalt porphyrin monomers display only one Co(III/II) wave and are poor catalysts.

Electrodes coated with electroactive polymers have been intensively researched over the past several years. Besides providing avenues for fundamental studies of the electroactive materials,[1] coated electrodes can have applications in energy storage, electrocatalysis, photosensitization, electrochromics, electroanalysis, and controlled ion release.[1c,2] The electroactive polymers include those prepared by electropolymerization of aniline,[3] phenol,[4] and pyrrole[5] and their derivatives; the electropolymerization chemistry of these monomers and the electrochemical, electrical, and physicochemical properties of their polymer films have been reported in the literature.

Attachment of metalloporphyrins to electrodes is attractive on several grounds. These molecules exhibit a rich electron-transfer chemistry, are ingredients of biopolymers, can often be manipulated by axial ligation to the central metal ion, and are potentially good catalysts and photosensitizers. Previous immobilization studies of porphyrins and phthalocyanines have relied on chemisorption,[6] vapor deposition,[7] and condensation reactions of porphyrin side chains with functionalized electrodes.[8] Polymeric porphyrin films have been obtained by amidization or esterification of a methyl acryl polymer and subsequent adsorption of the polymer–porphyrin solution[9] and by the uptake of charged porphyrins by ion-exchange polymer coatings.[10] Macor and Spiro used a different approach by oxidatively electropolymerizing metal/protoporphyrin IX complexes via the vinyl substituents on the porphyrin periphery.[11]

Following our own experiences with amino-substituted ruthenium phenanthroline complexes,[12] we recently investigated and reported on the oxidative electropolymerization of tetrakis(*o*-aminophenyl)porphyrin (H_2(*o*-NH_2)TPP) and some of its metalated derivatives.[13] The electropolymerized poly-Co(*o*-NH_2)TPP films are effective catalysts for the electroreduction of dioxygen in aqueous solutions,[14] and in general the electropolymerized porphyrin films have proved to be stable, adherent, and electroactive at the expected potentials.[13]

We report here a broadened electrochemical and spectroscopic study of porphyrin electrooxidative polymerization using amino-, dimethylamino-, and hydroxy-substituted tetraphenylporphyrins, their cobalt and nickel complexes, and a newly synthesized porphyrin, tetrakis(*p*-*N*-pyrrolylphenyl)porphyrin (H_2(*p*-pyr)TPP) that was designed to electropolymerize via polypyrrole-like couplings.[5] Spiro et al.[15] are also investigating some of these compounds, particularly their spectroscopy. Dioxygen catalysis by the cobalt porphyrin films is compared to that by the previously studied[14] poly-Co(*o*-NH_2)TPP. An example of catalytic H_2 evolution is included.

* To whom correspondence should be addressed.
† On sabbatical leave from the Nuclear Research Center, Negev, Beer-Sheva, Israel.
‡ Present address: Department of Chemistry, Massachusetts Institute of Technology, Cambridge, MA 02139.

(1) (a) Andrieux, C. P.; Bouchiat, J. M. O.; Saveant, J. M. *J. Electroanal. Chem. Interfacial Electrochem.* **1984**, *169*, 9. (b) Martin, C. R.; Rubinstein, I.; Bard, A. J. *J. Am. Chem. Soc.* **1982**, *104*, 4817. (c) Murray, R. W. *Annu. Rev. Mater. Sci.* **1984**, *14*, 145.

(2) (a) Murray, R. W. *Electroanal. Chem.* **1984**, *13*, 191–368. (b) Wrighton, M. S. In *Catalysis and Electrocatalysis*; Miller, J. S., Ed.; ACS Symposium Series 192; American Chemical Society: Washington, DC, 1982, p 99. (c) Zinger, B.; Miller, L. L. *J. Am. Chem. Soc.* **1984**, *106*, 6861. (d) Wrighton, M. S. *Science (Washington, D.C.)* **1986**, *231*, 32. (e) Chidsey, C. E. D.; Murray, R. W. *Science (Washington, D.C.)* **1986**, *231*, 25.

(3) (a) Diaz, A. F.; Logan, J. A. *J. Electroanal. Chem. Interfacial Electrochem.* **1980**, *111*, 111. (b) Noufi, R.; Nozik, A. J.; White, J.; Warren, L. F. *J. Electrochem. Soc.* **1982**, *129*, 2261. (c) Kobayashi, T.; Yoneyama, H.; Tamura, H. *J. Electroanal. Chem. Interfacial Electrochem.* **1984**, *161*, 419. (d) Ohsaka, T.; Ohnuki, Y.; Oyama, N.; Katagiri, G.; Kamisako, K. *J. Electroanal. Chem. Interfacial Electrochem.* **1984**, *161*, 399. (e) Mohilner, D. M.; Adams, R. N.; Argersinger, W. J., Jr. *J. Am. Chem. Soc.* **1962**, *84*, 3618. (f) McManus, P. M.; Yang, S. C.; Cushman, R. *J. Chem. Soc., Chem. Commun.* **1985**, *1556*. (g) Chiang, J.-C.; Macdiarmid, A. G. *Synth. Met.* **1986**, *13*, 193.

(4) (a) Mourcel, P.; Pham, M.-C.; Lacaze, P.-C.; Dubois, J.-E. *J. Electroanal. Chem. Interfacial Electrochem.* **1983**, *145*, 467. (b) Ohnuki, Y.; Matsuda, H.; Ohsaka, T.; Oyama, N. *J. Electroanal. Chem. Interfacial Electrochem.* **1983**, *158*, 55. (c) Dubois, J.-E.; Lacaze, P.-C.; Pham, M. C. *J. Electroanal. Chem. Interfacial Electrochem.* **1981**, *117*, 233. (d) Lapkowski, M.; Zak, J.; Strojek, J. W. *J. Electroanal. Chem. Interfacial Electrochem.* **1983**, *145*, 173. (e) Cheek, G.; Wales, C. P.; Nowak, R. *Anal. Chem.* **1983**, *55*, 380. (f) Finklea, H. O.; Vithange, R. S. *J. Electroanal. Chem. Interfacial Electrochem.* **1984**, *161*, 283. (g) Bruno, F.; Pham, M. C.; Dubois, J.-E. *Electrochim. Acta* **1977**, *22*, 451.

(5) (a) Bull, R. A.; Fan, F.-R.; Bard, A. J. *J. Electrochem. Soc.* **1983**, *130*, 1636. (b) Skotheim, T.; Lundstrom, I.; Praza, J. *J. Electrochem. Soc.* **1981**, *128*, 1625. (c) Frank, A. J.; Honda, K. *J. Phys. Chem.* **1982**, *86*, 1933. (d) Burgmayer, P.; Murray, R. W. *J. Electroanal. Chem. Interfacial Electrochem.* **1983**, *147*, 339. (e) Tourillon, G.; Garnier, F. *J. Electroanal. Chem. Interfacial Electrochem.* **1982**, *135*, 173. (f) Pickup, P. G.; Osteryoung, R. A. *J. Am. Chem. Soc.* **1984**, *106*, 2294. (g) Genies, E. M.; Bidan, G.; Diaz, A. F. *J. Electroanal. Chem. Interfacial Electrochem.* **1983**, *149*, 101. (h) Kanazawa, K. K.; Diaz, A. F.; Geiss, R. H.; Gill, W. D.; Kwak, K. F.; Logan, J. A. *J. Chem. Soc., Chem. Commun.* **1979**, 854. (i) Diaz, A. F.; Castillo, J.; Kanazawa, K. K.; Logan, J. A. *J. Electroanal. Chem. Interfacial Electrochem.* **1982**, *133*, 233. (j) Diaz, A. F.; Castillo, J. *J. Chem. Soc., Chem. Commun.* **1980**, 397.

(6) (a) Bettelheim, A.; Chan, R. J. H.; Kuwana, T. *J. Electroanal. Chem. Interfacial Electrochem.* **1979**, *99*, 391. (b) Zagal, J.; Sen, R. K.; Yeager, E. *J. Electroanal. Chem. Interfacial Electrochem.* **1977**, *83*, 207. (c) Collman, J. P.; Denisevich, P.; Konai, Y.; Morrocco, M.; Koval, C.; Anson, F. C. *J. Am. Chem. Soc.* **1980**, *102*, 6027. (d) Durand, R. R.; Anson, F. C. *J. Electroanal. Chem. Interfacial Electrochem.* **1982**, *134*, 273. (e) Durand, R. R.; Bencosme, C. S.; Collman, J. P.; Anson, F. C. *J. Am. Chem. Soc.* **1983**, *105*, 2710. (f) Liu, H.-Y.; Abdalmuhdi, I.; Chang, C. K.; Anson, F. C. *J. Phys. Chem.* **1985**, *89*, 665. (g) Shigehara, K.; Anson, F. C. *J. Phys. Chem.* **1982**, *86*, 2776.

(7) (a) Tachikawa, H.; Faulkner, L. *J. Am. Chem. Soc.* **1978**, *100*, 4379. (b) Jaeger, C.; Fan, F.; Bard, A. J. *J. Am. Chem. Soc.* **1980**, *102*, 2592.

0020-1669/87/1326-1009$01.50/0

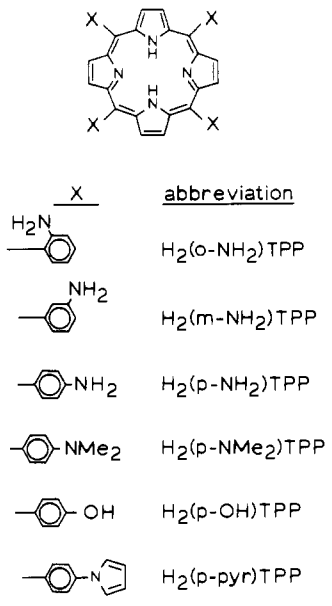

Figure 1. Structures and abbreviations of porphyrins used in this study.

Experimental Section

Preparation of Porphyrins and Metalloporphyrin Complexes. The structures of the porphyrins and our abbreviations of them are shown in Figure 1.

H_2(*p*-NO_2)TPP.[16] An 11.0-g (73-mmol) amount of *p*-nitrobenzaldehyde and 12.0 mL (127 mmol) of acetic anhydride were added to 300 mL of stirring propionic acid, and the resulting solution was brought to reflux. A 5.0-mL (73-mmol) amount of freshly distilled pyrrole in 10 mL of propionic acid was added and the mixture refluxed for 30 min with stirring. The tarry solution was allowed to cool and stand for 24 h. A dark solid was collected by filtration, washed with six 100-mL portions of H_2O, and dried. The powdery solid was taken up in 80 mL of pyridine, refluxed with stirring for 1 h, cooled to room temperature, and then stored at −4 °C overnight. The tarry mixture was filtered and the solid product washed repeatedly with acetone until the rinsings were no longer dark; yield 2.7–3.2 g (19–22%). This procedure can be scaled up (4-fold) with no decrease in yield.

H_2(*p*-NH_2)TPP.[17] A solution of 2.0 g (2.5 mmol) of H_2(*p*-NO_2)TPP in 100 mL of concentrated HCl was bubbled with Ar for 1 h. A solution of 9.0 g (40 mmol) of $SnCl_2 \cdot 2H_2O$ in 140–15 mL of concentrated HCl, also bubbled with Ar, was added to the porphyrin solution, which was stirred and heated in a water bath (75–80 °C) for 30 min. The hot-water bath was carefully replaced by a cold-water bath and then an ice bath. The reaction mixture was then neutralized under Ar by slow addition of 125 mL of concentrated NH_4OH, taking care to maintain a low temperature throughout the very exothermic reaction. The resultant basic solution was exposed to air and filtered and the greenish solid stirred vigorously with 200 mL of 5% NaOH. The solid was again filtered, washed with H_2O, dried, and then Soxhlet extracted with 250 mL of $CHCl_3$. The volume of the purple solution was reduced to 150 mL by rotary evaporation. Addition of 100 mL of 95% EtOH and slow rotary evaporation gave crystalline H_2(*p*-NH_2)TPP, yield about 1.0 g (40–60%).

H_2(*m*-NO_2)TPP. A 27.5-g (182-mmol) amount of *m*-nitrobenzaldehyde and 30 mL (318 mmol) of acetic anhydride were added to 850 mL of stirring propionic acid. After the solution was brought to reflux, 12.5 mL (182 mmol) of freshly distilled pyrrole in 50 mL of propionic acid was added and the reflux continued, with stirring, for 45 min. The reaction mixture was allowed to cool and stand overnight. The dark solid was collected by filtration, washed with water, and dried. An insulated Soxhlet apparatus was used to extract the product into 500 mL of toluene, which was taken to dryness by rotary evaporation. The residue was dissolved in 300 mL of CH_2Cl_2 to which 150–200 mL of silica gel (Grace Grade 62) was added, stirred, removed by filtration, and washed repeatedly with CH_2Cl_2 until the rinsings were pale. The large volume of purple CH_2Cl_2 solution was reduced by rotary evaporation to 75 mL; addition of 200 mL of MeOH and further rotary evaporation precipitated H_2(*m*-NO_2)TPP, yield 1.4 g (4%).

H_2(*m*-NH_2)TPP. Reduction of H_2(*m*-NO_2)TPP was carried out as described for the *para* isomer; yield 40–60%.

H_2(*p*-pyr)TPP.[18] A 25-mL amount of glacial acetic acid was added to 200 mg (151 mmol) of 2,5-dimethoxytetrahydrofuran (Aldrich) and 200 mg (3.30 mmol) of H_2(*p*-NH_2)TPP and the resultant solution refluxed with stirring for 1.5 h. A precipitate formed during the reaction. After the mixture was cooled to room temperature, the porphyrin was filtered and washed with methanol and hexane; yield 200 mg (75%). The completeness of the reaction was checked by using IR spectroscopy in KBr pellets. No maxima at about 3400 cm^{-1} were observed for the final product, indicating the absence of stretching vibration for free aromatic amine groups.

H_2(*o*-NH_2)TPP was synthesized according to a published procedure.[19] H_2(*p*-NMe_2)TPP and H_2(*p*-OH)TPP were obtained from Midcentury Chemicals (Posen, IL). Metalations were accomplished in refluxing dimethylformamide.[20] Cobalt(III) porphyrins resulted from refluxing in the presence of air for 2–3 h. Completeness of metalation was checked by visible spectroscopy. Metalation with cobalt was also achieved by reacting electropolymerized free base films on electrodes at 50 °C with a tetrahydrofuran solution containing 0.1 M $CoCl_2$.

Materials, Electrodes, and Instrumentation. Tetraethylammonium perchlorate (Et_4NClO_4) was twice recrystallized from water and tetrabutylammonium perchlorate (Bu_4NClO_4) once from ethyl acetate. Spectroquality acetonitrile (Burdick and Jackson) and methylene chloride (Baker) were stored over 4-Å molecular sieves. Teflon-shrouded glassy-carbon (GC, Atomergic Chemicals) and Pt working electrodes were polished with 1-μm diamond paste (Buehler). SnO_2 films on glass served as optically transparent electrodes. Potentials are reported vs. a Ag/(saturated KCl)AgCl reference electrode. Electrochemical experiments were conducted with conventional three-electrode cells and instrumentation. Visible absorption spectra were acquired with a Tracor Northern TN-1710A or a Hewlett-Packard 8450A UV/vis spectrophotometer; IR spectra for porphyrins in KBr pellets and of electropolymerized films on SnO_2 electrodes were acquired with a Nicolet 5DXP.

Electropolymerizations. These were accomplished from 0.1 M Et_4NClO_4/CH_3CN or 0.1 M Bu_4NClO_4/CH_2Cl_2 solutions containing 0.7–1.0 mM porphyrin or metalloporphyrin monomer by cyclically scanning (200 mV/s) the working-electrode potential between 0 V and a positive potential, as listed in Table III. The quantity of electrodeposited, electroactive porphyrin, or film coverage, Γ (mol/cm^2), was determined by integration of the charge under the cyclic voltammetric waves observed in deaereated 0.1 M Et_4NClO_4/CH_3CN. The counterions of the cobalt porphyrin polymers are not known with certainty. For example, the cobalt porphyrins are electropolymerized from the chloride monomer salts, but during subsequent electrochemical reductions in perchlorate electrolyte to Co(I) states chloride may be lost from the film.

Results and Discussion

Absorption Spectroscopy of Dissolved Porphyrins. In a previous publication,[14] we suggested that the multiple electrochemical and electrocatalytic O_2 reduction waves observed for both solutions and electropolymerized films of Co^{III}(*o*-NH_2)TPP(Cl) might arise from mixtures of monomeric and dimeric (or higher aggregate)

(8) (a) Jester, C. P.; Rocklin, R. D.; Murray, R. W. *J. Electrochem. Soc.* **1980**, *127*, 1979. (b) Willman, K. W.; Rocklin, R. D.; Nowak, R.; Kuo, K. N.; Schultz, F. A.; Murray, R. W. *J. Am. Chem. Soc.* **1980**, *102*, 7629. (c) Elliott, C. M.; Marresse, C. A. *J. Electroanal. Chem. Interfacial Electrochem.* **1981**, *119*, 395.
(9) Bettelheim, A.; Chan, R. J. H.; Kuwana, T. *J. Electroanal. Chem. Interfacial Electrochem.* **1980**, *110*, 93.
(10) (a) Buttry, D. A.; Anson, F. C. *J. Am. Chem. Soc.* **1984**, *106*, 59. (b) Anson, F. C.; Ni, C. L.; Saveant, J. M. *J. Am. Chem. Soc.* **1985**, *107*, 3442.
(11) (a) Macor, K. A.; Spiro, J. G. *J. Am. Chem. Soc.* **1983**, *105*, 5601. (b) Macor, K. A.; Spiro, T. G. *J. Electroanal. Chem. Interfacial Electrochem.* **1984**, *163*, 223.
(12) Ellis, C. D.; Margerum, C. D.; Murray, R. W.; Meyer, T. J. *Inorg. Chem.* **1983**, *22*, 1283.
(13) White, B. A.; Murray, R. W. *J. Electroanal. Chem. Interfacial Electrochem.* **1985**, *189*, 345.
(14) Bettelheim, A.; White, B. A.; Murray, R. W. *J. Electroanal. Chem. Interfacial Electrochem.* in press.
(15) Su, Y. O.; Macor, K. A.; Miller, L. A.; Spiro, T. G. Presented at the 191st National Meeting of the American Chemical Society, New York City, April 1986; Abstract INOR 50.
(16) Semeikin, A. S.; Koifman, O. I.; Berezin, B. D. *Khim. Geterotsikl. Soedin.* **1982**, *10*, 1354.
(17) Sorrell, T. N. *Inorg. Synth.* **1980**, *20*, 163.
(18) Elming, N.; Clauson-Kaas, N. *Acta Chem. Scand.* **1952**, *6*, 867.
(19) Collman, J. P.; Gagne, R. R.; Reed, C. A.; Halbert, T. R.; Land, G.; Robinson, W. T. *J. Am. Chem. Soc.* **1975**, *97*, 1427.
(20) Adler, A. D.; Longo, F. R.; Kampas, F.; Kim, J. *J. Inorg. Nucl. Chem.* **1970**, *32*, 2443.

Table I. Visible Absorption Data for Free-Base and Co(III) Porphyrins

compd	concn, M	solvent	electrolyte[a]	λ_{max}, nm
H_2(*o*-NH_2)TPP	1.4×10^{-6}–2.2×10^{-5}	CH_2Cl_2	Bu_4NClO_4	416, 514, 548, 588, 646
H_2(*m*-NH_2)TPP	1.5×10^{-6}–2.0×10^{-5}	CH_2Cl_2	none	420, 514, 550, 590, 646
H_2(*p*-NH_2)TPP	1.5×10^{-6}–2.3×10^{-5}	CH_2Cl_2	Bu_4NClO_4	428, 460, 520, 562, 656
H_2(*p*-NMe_2)TPP	2.5×10^{-6}–3.8×10^{-5}	CH_2Cl_2	Bu_4NClO_4	399, 438, 470, 514, 570, 670
H_2(*p*-OH)TPP[b]	1.4×10^{-6}–2.2×10^{-5}	aqueous	NaOH	434, 594–600, 660–676
H_2(*p*-pyr)TPP	1.5×10^{-6}–2.0×10^{-5}	CH_2Cl_2	Bu_4NClO_4	422, 518, 550, 590, 646
Co(*o*-NH_2)TPP	1.4×10^{-5}	CH_2Cl_2	none	412, 432, 546
	6.9×10^{-5}	CH_2Cl_2	none	408, 528
	2.7×10^{-6}	CH_2Cl_2	Bu_4NClO_4	416, 434, 546
	5.5×10^{-6}–2.2×10^{-5}	CH_2Cl_2	Bu_4NClO_4	410, 530
	5.5×10^{-7}–8.3×10^{-6}	Me_2SO	Bu_4NClO_4	430,[f] 546
	1.4×10^{-6}–2.2×10^{-5}	aqueous	$HClO_4$	420,[h] 536
	1.4×10^{-6}–2.2×10^{-5}	aqueous	H_2SO_4	420,[i] 536
Co(*m*-NH_2)TPP	5.5×10^{-7}–8.3×10^{-6}	Me_2SO	Bu_4NClO_4	436,[d] 548
Co(*p*-NH_2)TPP	5.5×10^{-7}–8.3×10^{-6}	Me_2SO	Bu_4NClO_4	440,[e] 552, 598
Co(*p*-NMe_2)TPP	1.9×10^{-5}	CH_2Cl_2	none	440, 536, 574[k]
	1.9×10^{-6}–4.5×10^{-5}	CH_2Cl_2	Bu_4NClO_4	434–428,[c] 536, 574[k]
Co(*p*-OH)TPP	1.6×10^{-5}	CH_3CN	none	414, 430, 542, 590 (sh)
	1.4×10^{-6}	CH_3CN	Et_4NClO_4	434, 552, 592 (sh)
	5.4×10^{-6}–2.2×10^{-5}	CH_3CN	Et_4NClO_4	416, 430, 546, 590 (sh)
	1.4×10^{-6}–2.2×10^{-5}	aqueous	NaOH	440,[j] 562, 608
Co(*p*-pyr)TPP	10^{-5}	CH_2Cl_2	none	434, 552, 590
	2.5×10^{-6}–2.0×10^{-5}	CH_2Cl_2	Bu_4NClO_4	414, 434, 544–532, 590
	5.0×10^{-7}–7.5×10^{-6}	Me_2SO	Bu_4NClO_4	432,[g] 546, 590

[a] Electrolytes in organic solvents were 0.1 M Bu_4NClO_4 and Et_4NClO_4; those in aqueous solutions were 1 M $HClO_4$, 0.5 M H_2SO_4, and 1 M NaOH. [b] H_2(*p*-OH)TPP is insoluble in CH_2Cl_2 and CH_3CN. [c] Beer's law obeyed although peak shifts from 434 to 428 nm with increasing concentration; $\epsilon_{max} = 2.3 \times 10^4$ M^{-1} cm^{-1}. [d] Beer's law obeyed; $\epsilon_{max} = 5.0 \times 10^4$ M^{-1} cm^{-1}; only one Soret band observed; insoluble in CH_2Cl_2. [e] Beer's law obeyed; ϵ_{max} v 1.2×10^5 M^{-1} cm^{-1}; only one Soret band observed; insoluble in CH_2Cl_2. [f] Beer's law obeyed; $\epsilon_{max} = 6.7 \times 10^4$ M^{-1} cm^{-1}; only one Soret band observed. [g] Beer's law obeyed; $\epsilon_{max} = 6.2 \times 10^4$ M^{-1} cm^{-1}; only one Soret band observed. [h] Beer's law obeyed; $\epsilon_{max} = 1.2 \times 10^5$ M^{-1} cm^{-1}; only one Soret band observed. [i] Beer's law obeyed; $\epsilon_{max} = 1.3 \times 1^5$ M^{-1} cm^{-1}; only one Soret band observed. [j] Beer's law obeyed; $\epsilon_{max} = 1.2 \times 10^5$ M^{-1} cm^{-1}; only one Soret band observed. [k] Poorly defined peak.

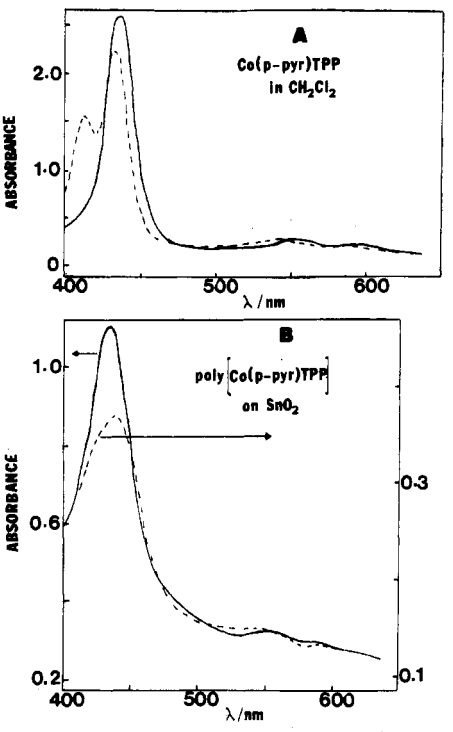

Figure 2. (A) Spectra for 10^{-5} M Co(*p*-pyr)TPP in CH_2Cl_2 in the absence (solid curve) and presence (dashed curve) of 0.1 M Bu_4NClO_4. (B) Spectra for poly-Co(*p*-pyr)TPP film on SnO_2. The solid curve is for a film produced by electropolymerization of Co(*p*-pyr)TPP, and the dashed curve is for a film of poly-Co(*p*-pyr)TPP produced by insertion of cobalt ions into poly-H_2(*p*-pyr)TPP.

species. Seeking supporting evidence for aggregation, we have examined the effects of porphyrin concentration, electrolyte, and solvent on the visible spectroscopy of the cobalt and the free-base porphyrins that we have been able to electropolymerize.

Spectra of the free-base porphyrins in CH_2Cl_2 containing 0.1 M Bu_4NClO_4 over the 400–700-nm range give typical porphyrin spectra, with one very intense absorption band at about 415–440 nm that obeys Beer's law and up to four bands at longer wavelength of much lower intensity (Table I). The spectrum of H_2(*p*-NMe_2)TPP is unusual in that two Soret bands are observed (399 and 438 nm).

As for the cobalt porphyrins, in the coordinating solvents Me_2SO and water, Co(*m*-NH_2)TPP(Cl), Co(*p*-NH_2)TPP(Cl), Co(*o*-NH_2)TPP(Cl), Co(ppyr)TPP(Cl), and Co(*p*-OH)TPP(Cl) exhibit single Soret peaks in the 420–440-nm range that obey Beer's law over the concentration ranges indicated in Table I. Molar absorbance coefficients are given in the Table footnotes.

In poorly coordinating solvents, on the other hand, we observed shifts in λ_{max} and splitting of Soret peaks that were dependent on the cobalt porphyrin concentration and on the presence of the perchlorate electrolyte. The effect of added electrolyte is illustrated in Figure 2A, where the λ_{max} = 436 nm Soret band for 10^{-5} M Co(*p*-pyr)TPP(Cl) in CH_2Cl_2 solution is split (λ_{max} = 414, 434 nm) by adding 0.1 M Bu_4NClO_4. The weak, longer wavelength bands are also shifted (552 to 542 nm in Figure 2A). The λ_{max} absorbances of the 414- and 434-nm peaks for Co(*p*-pyr)TPP(Cl) in 0.1 M Bu_4NClO_4 do not vary linearly with porphyrin concentration, as shown in Figure 3A. Variation in absorbance ratios (Figure 3B) further indicates that the 434- and 414-nm peaks are the prominent bands at low and high porphyrin concentrations, respectively.

We ascribe the spectral changes for Co(*p*-pyr)TPP to a porphyrin aggregation process analogous to those known[21] for porphyrins in the absence of strongly coordinating ligands. The

(21) (a) Abraham, R. J. *Proc. Chem. Soc., London* **1963**, 134. (b) McCragh, A.; Storm, C. B.; Koshi, W. S. *J. Am. Chem. Soc.* **1965**, *87*, 1470. (c) Mauzerall, D. *Biochemistry* **1965**, *4*, 1801. (d) Dougherty, D. A.; Dwiggins, C. W., Jr. *J. Phys. Chem.* **1969**, *73*, 423. (e) Storm, C. B.; Corwin, A. H.; Arellano, R. R.; Martz, M.; Weintraub, R. *J. Am. Chem. Soc.* **1966**, *88*, 2525. (f) Das, R. R.; Pasternack, R. F.; Plane, R. A. *J. Am. Chem. Soc.* **1970**, *92*, 3312. (g) Pasternack, R. F.; Huber, P. R.; Boyd, P.; Eugassen, G.; Francesconi, L.; Gibbs, E.; Fasella, P.; Venturo, G. C.; de C. Hinds, L. *J. Am. Chem. Soc.* **1972**, *94*, 4511. (h) Hill, H. A. O.; Sadler, P. J.; Williams, R. J. P. *J. Chem. Soc., Dalton Trans.* **1973**, 1663. (i) Pasternack, R. F.; Francesconi, L.; Raff, D.; Spiro, E. *Inorg. Chem.* **1973**, *12*, 2606. (j) Walker, F. A. *J. Magn. Reson.* **1974**, *15*, 201.

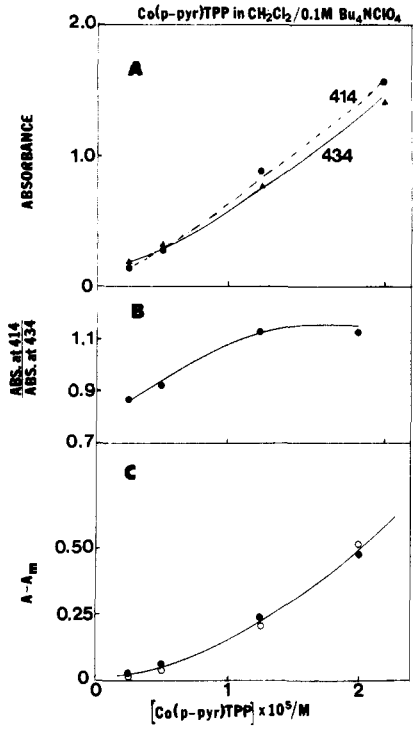

Figure 3. (A) Absorbance at λ_{max} = 414 and 434 nm vs. Co(*p*-pyr)TPP concentration of Co(*p*-pyr)TPP in 0.1 M Bu_4NClO_4/CH_2Cl_2. (B) Ratio of absorbances in (A) vs. Co(*p*-pyr)TPP concentration. (C) Fit of (A) data to eq 2. The points are calculated from eq 2 and ϵ_D and K_D values given in Table II (○) and experimental values (●).

absorbance data were analyzed in terms of a dimerization model where λ_{max} = 434 nm represents absorbance by monomer in the absence of electrolyte and λ_{max} = 414 nm represents that by dimer formed in the presence of electrolyte and/or at high porphyrin concentration

$$2\text{Co}(p\text{-pyr})\text{TPP} \rightleftarrows [\text{Co}(p\text{-pyr})\text{TPP}]_2 \quad (1)$$

according to the equation[20g]

$$A_m - A = ((2\epsilon_M - \epsilon_D)(4K_D C_{Co} + 1 - [1 + 8K_D C_{Co}]^{1/2}))/8K_D \quad (2)$$

where C_{Co} is total porphyrin concentration, $A_m = \epsilon_M C_{Co}$ is the absorption the solution would have at the monomer wavelength (434 nm) in the absence of aggregation, A is the absorbance actually measured at the monomer wavelength, ϵ_M and ϵ_D are the molar absorptivities of monomer and dimer, respectively, and K_D is the dimerization equilibrium constant (e.g., $[\text{Co}(p\text{-pyr})\text{TPP}]_2/[\text{Co}(p\text{-pyr})\text{TPP}]^2$) at constant ionic strength, μ = 0.1 M. $\epsilon_M = 5.2 \times 10^4$ M^{-1} cm^{-1} at 434 nm from spectra obtained at low porphyrin concentration and absence of electrolyte, and after curve fitting as illustrated in Figure 3C, we obtain $\epsilon_D = 2.2 \times 10^5$ M^{-1} cm^{-1} for the dimer at 414 nm and $K_D = 3 \times 10^4$ M^{-1} for the dimerization of Co(*p*-pyr)TPP in CH_2Cl_2. The same analysis was followed for Co(*o*-NH_2)TPP and Co(*p*-OH)TPP solutions, which exhibited similar Soret splittings, with data summarized in Table II. (Being insoluble in CH_2Cl_2, Co(*p*-OH)TPP was studied in CH_3CN.) In 0.1 M Bu_4NClO_4/CH_2Cl_2, the dimerization constant for Co(*o*-NH_2)TPP (6×10^6 M^{-1}) is 2 orders of magnitude larger than for Co(*p*-pyr)TPP (3×10^4 M^{-1}). The large K_D for Co(*o*-NH_2)TPP is also consistent with the appearance of a split Soret peak for this compound in CH_2Cl_2 even in the absence of electrolyte (Table I). Dimerization of Co(*p*-NMe_2)TPP in 0.1 M Bu_4NClO_4/CH_2Cl_2 is apparently quite weak since the Soret shifts only slightly with concentration and does not split (Table I), and the Co(*m*-NH_2)TPP and Co(*p*-NH_2)TPP isomers were insoluble in CH_2Cl_2 and were not studied.

These results collectively suggest that both the presence of electrolyte and the amine and hydroxy substituents help to promote aggregation of these porphyrins. Spiro et al.[15] have come to a similar conclusion on the basis of a differing set of experiments. The effects can be rationalized by intermolecular axial coordination by the amine and hydroxy groups plus metal–metal axial bridging interactions induced by perchlorate. Thus, the aggregation is weakened or broken by dimethylation of the amine (as in Co(*p*-NMe_2)TPP), use of benign substituents (as pyrrole in Co(*p*-pyr)TPP), or use of polar, axially coordinating solvents (as in Me_2SO or water).

Table II. Dimerization Constants (K_D) and Molar Absorptivities of the Monomer (ϵ_M) and Dimer (ϵ_D) for Cobalt Porphyrins

compd	solvent	ϵ_M^{434},[a] M^{-1} cm^{-1}	ϵ_D^{414},[b] M^{-1} cm^{-1}	K_D,[b] M^{-1}
Co(*o*-NH_2)TPP	CH_2Cl_2	5.9×10^4	1.9×10^5	6×10^6
Co(*p*-OH)TPP	CH_3CN	3.6×10^4	9.3×10^4	1×10^6
Co(*p*-pyr)TPP	CH_2Cl_2	5.2×10^4	2.2×10^5	3×10^4

[a] The molar absorptivities at 414 nm were calculated from the spectroscopic data at low concentrations of Co(*p*-OH)TPP and Co(*p*-pyr)TPP in CH_3CN and CH_2Cl_2, respectively. ϵ_M for Co(*o*-NH_2)TPP was taken from spectra in Me_2SO and assumed to be the same in CH_2Cl_2. [b] Calculated as in Figure 3C for the cobalt porphyrin dissolved in CH_2Cl_2 or CH_3CN in the presence of 0.1 M Bu_4NClO_4 and Et_4NClO_4, respectively.

Electrochemistry of Dissolved Porphyrins. Formal potentials obtained for reductions by cyclic voltammetry (Pt and GC electrodes) of free-base, Co(III), and Ni(II) porphyrin solutions are summarized in Table III. Since polymerization accompanies oxidation of these porphyrins, $E^{\circ\prime}$ values for oxidations are not readily obtained.

For the free-base porphyrins, the one-electron reductions to the anion radicals occur in uncomplicated, reversible waves. Reductions to dianions occur at more negative potentials (not shown in Table III). Kadish et al. have shown[22] that formal potentials for $H_2(p\text{-X})\text{TPP}^{0/\bullet-}$ couples vary with the electron donation/withdrawal properties of X. Comparing the formal potentials in CH_2Cl_2/Bu_4NClO_4 of $H_2\text{TPP}^{0/\bullet-}$ (−1.28 V), $H_2(o\text{-NH}_2)\text{TPP}^{0/\bullet-}$ (−1.26 V), $H_2(m\text{-NH}_2)\text{TPP}^{0/\bullet-}$ (−1.32 V), and $H_2(p\text{-NH}_2)\text{TPP}^{0/\bullet-}$ (−1.35 V) (Table III) reveals that the electronic influence of the amino group varies substantially with its *position* on the phenyl ring, the apparent electron donation increasing in the order *o*-NH_2 < *m*-NH_2 < *p*-NH_2.

The reduction of Ni(II) porphyrins is ligand-centered;[22] $Ni^{II}\text{TPP}$ is reported[23] to be reduced to $Ni^{II}(\text{TPP}^{\bullet-})$ and to $Ni^{II}(\text{TPP}^{2-})$ at −1.18 and −1.75 V vs. SCE in DMF/C_6H_6. These values are similar to those obtained for Ni(*o*-NH_2)TPP in CH_3CN (−1.24 and −1.73 V). Ni(*p*-OH)TPP is, however, reduced at less negative potentials (−0.86 and −1.38 V); some special reduced-ligand stabilizing factor seems to be turned on by the hydroxy groups.

The first reduction steps seen for the cobalt porphyrins are in the $E^{\circ\prime} = -0.9$ V range (Table III) that has been[23,24] attributed to the formation of Co(I). The ca. 0.1 mM concentrations used should promote aggregation (vide supra), and the Co(II/I) $E^{\circ\prime}$ values will include this as well as substituent effects. No clear Co(III) → Co(II) wave was observed in CH_2Cl_2 or CH_3CN for any of the cobalt porphyrins listed in Table III. Oxidation potentials for Co(II) porphyrins are strongly affected by axial coordination;[25] facile oxidation of Co^{II} (*p*-X)TPP to Co^{III}(*p*-X)TPP occurs in strongly coordinating solvents like Me_2SO and pyridine, while in noncoordinating solvents like CH_2Cl_2, oxidation of Co(II) is shifted positively and becomes irreversible.[24a]

Electropolymerizations in Organic Solvents. Amino-Substituted Tetraphenylporphyrins. We described earlier[13,14] the oxidations of $H_2(o\text{-NH}_2)\text{TPP}$ and various metalated complexes that by repetitive potential scanning between 0.0 and +1.1 V produce adherent polymeric films (abbreviated poly-$H_2(o\text{-NH}_2)$TPP) on

(22) Kadish, K. M.; Morrison, M. M. *J. Am. Chem. Soc.* **1976**, *98*, 3326.
(23) Felton, R. H.; Linschitz, H. *J. Am. Chem. Soc.* **1966**, *88*, 1113.
(24) (a) Walker, F. A.; Beroiz, D.; Kadish, K. M. *J. Am. Chem. Soc.* **1976**, *98*, 3484. (b) Kellet, R. M.; Spiro, T. G. *Inorg. Chem.* **1985**, *24*, 2373.
(25) (a) Carter, M. J.; Englehardt, L. M.; Rillema, D. P.; Basolo, F. *J. Chem. Soc., Chem. Commun.* **1973**, 810. (b) Carter, M. J.; Rillema, D. P.; Basolo, F. *J. Am. Chem. Soc.* **1974**, *96*, 392.

Table III. Electrochemical Data for Solutions and Electropolymerized Films of Porphyrins and Metalloporphyrins

compd	solvent/electrolyte[a]	potential range for electropolymerizn,[b] V vs. Ag/AgCl	$E^{\circ\prime}$,[c] V vs. Ag/AgCl: redn soln	redn film	oxidn[d] soln	oxidn[d] film	Γ_{max},[e] mol/cm^2
H_2TPP	CH_2Cl_2/Bu_4NClO_4	0 → +1.1	−1.28				
H_2(*o*-NH_2)TPP	CH_3CN/Et_4NClO_4	0 → +1.1	−1.13	−1.09			10^{-8}
	CH_2Cl_2/Bu_4NClO_4	0 → +1.1	−1.26				
H_2(*m*-NH_2)TPP	CH_2Cl_2/Bu_4NClO_4	0 → +1.1	−1.32	−1.35			5×10^{-9}
H_2(*p*-NH_2)TPP	CH_3CN/Et_4NClO_4	0 → +1.0	−1.19	−1.20	+0.6		
	CH_2Cl_2/Bu_4NClO_4	0 → +1.0	−1.35				2×10^{-8}
H_2(*p*-NMe_2)TPP	CH_2Cl_2/Bu_4NClO_4	0 → +0.7	−0.97[f]	−1.00[f]	+0.35[f]		
			−1.33	−1.34	+0.49	+0.49	2×10^{-8}
H_2(*p*-OH)TPP	water/NaOH	0 → +0.5			+0.1[g]		*f*
H_2(*p*-pyr)TPP	CH_2Cl_2/Bu_4NClO_4	0 → +1.1	−1.08	−1.05[h]	+1.0		
			−1.20	−1.27			10^{-7}
Ni(*o*-NH_2)TPP	CH_3CN/Et_4NClO_4	0 → +1.0	−1.24	−1.25			10^{-8}
Ni(*p*-NH_2)TPP	CH_3CN/Et_4NClO_4	0 → +0.75	−1.29	−1.29		+1.05	2×10^{-8}
Ni(*p*-OH)TPP	CH_3CN/Et_4NClO_4	0 → +1.3	−0.86	−0.90[f]	+0.97		
			−1.38	−1.38			10^{-8}
Co(*o*-NH_2)TPP	CH_3CN/Et_4NClO_4	0 → +1.0	−0.82	−0.82	+0.8		2×10^{-8}
Co(*m*-NH_2)TPP	*i*	*i*	*i*	−0.90	*i*		10^{-9}
Co(*p*-NH_2)TPP	*i*	*i*	*i*	−0.90	*i*		10^{-9}
Co(*p*-NMe_2)TPP	CH_2Cl_2/Bu_4NClO_4	0 → +1.0	−0.90	−0.92	+0.58		2×10^{-8}
					+0.80	+0.85	
Co(*p*-OH)TPP	CH_3CN/Et_4NClO_4	0 → +1.40	−0.84	−0.78	+0.95[j]	+0.45[f]	2×10^{-8}
		0 → −1.5	−0.86			+0.45[f]	
Co(*p*-pyr)TPP	CH_2Cl_2/Bu_4NClO_4	0 → +1.1	−0.88	−0.91	+0.38		10^{-7}
					+0.90		

[a] These media were used to study the electrochemistry of the dissolved compounds and their electropolymerization; 0.1 M Et_4NClO_4/CH_3CN was used to study the electrochemistry of all films. [b] Potential was cyclically scanned over the indicated range at 200 mV/s. [c] Formal potentials for the dissolved and film redox couples observed when scanning from 0 V in the negative direction (reductions: 0 → −1.9 V for free-base and nickel porphyrins; 0 → −1.2 V for cobalt porphyrins) or in the positive direction (oxidations: 0 → +1.1 V). [d] In the positive-potential scans, most of the films show broad, overlapping waves rather than well-resolved, sharp electrochemical oxidations; $E^{\circ\prime}$ values are reported only for well-defined waves. [e] Approximate maximum surface coverage obtained. [f] Irreversible reduction or oxidation peak; value reported is $E_{p,c}$ or $E_{p,a}$. [g] The film is nonconductive. [h] The current for the wave with $E^{\circ\prime} = -1.05$ V decreases and that for $E^{\circ\prime} = -1.27$ N increases upon repetitive cycling, but a steady-state pattern is eventually obtained. [i] Due to insolubility in CH_3CN and CH_2Cl_2, no electrochemistry or electropolymerizations could be performed. Poly-Co(*m*-NH_2)TPP and poly-Co(*p*-NH_2)TPP films were obtained by inserting cobalt ions into poly-H_2(*n*-NH_2)TPP and poly-H_2(*p*-NH_2)TPP films. [j] $E^{\circ\prime}$ value for main wave.

Pt or GC electrode surfaces. Analogous results for film-growth patterns seen in the electropolymerization of H_2(*m*-NH_2)TPP, H_2(*p*-NH_2)TPP, and H_2(*p*-NMe_2)TPP are shown in Figure 4. As is characteristic of nonpassivating electropolymerization, the polymer film remains electroactive at the electropolymerization potential so that the oxidation and reduction current envelope grows with each successive potential cycle. Following a previous study of amino-substituted ruthenium polypyridine complexes,[12] we attribute the electrooxidative film formation to aniline- (or N-substituted-aniline-) like polymerization[3] where porphyrin-substituted aromatic amine radical cations couple with one another. The complex current/potential patterns in Figure 4 vary somewhat with potential scan limits and rate, and we have not pursued a detailed analysis of the growth patterns. However, some general observations are possible.

On the basis of Hammett free energy relationships that predict[22] redox potentials for forming radical anions and cations from the free-base tetrakis(aminophenyl)porphyrins, it is clear that oxidation to porphyrin cation radicals can occur within the potentials scanned during electropolymerization (0 → 1.1 V). The chemistry of the aminophenyl substituents dominates the electrochemical behavior, however, and it appears that the substituents are oxidized concurrently with, or slightly before, the macrocyclic ring. For example, in the oxidation of H_2(*o*-NH_2)TPP, the chemically irreversible anodic current peak at +0.9 V recorded on the first scan is ca. 4× larger than that for the reversible, one-electron reduction to H_2(*o*-NH_2)TPP$^{\bullet-}$. This is consistent with a multielectron oxidation reaction and the presence of multiple amine sites. Moreover, the oxidation peaks seen in the first positive-potential scans in H_2(*p*-NH_2)TPP and H_2(*p*-NMe_2)TPP solutions (Figure 4B,C) occur at potentials (+0.5–0.6 V) less positive than those required for porphyrin ring oxidation and are more reasonably attributed to aminophenyl oxidation.

For all the free-base tetrakis(aminophenyl)porphyrins, the first oxidizing potential sweep is unique and is not repeated on subsequent scans. Instead, after several scans, a growth of a current envelope appears for a new couple in the electroactive film, for H_2(*o*-NH_2)TPP at about +0.8 V[13] and at about +0.5 V for H_2(*m*-NH_2)TPP, H_2(*p*-NH_2)TPP, and H_2(*p*-NMe_2)TPP (Figure

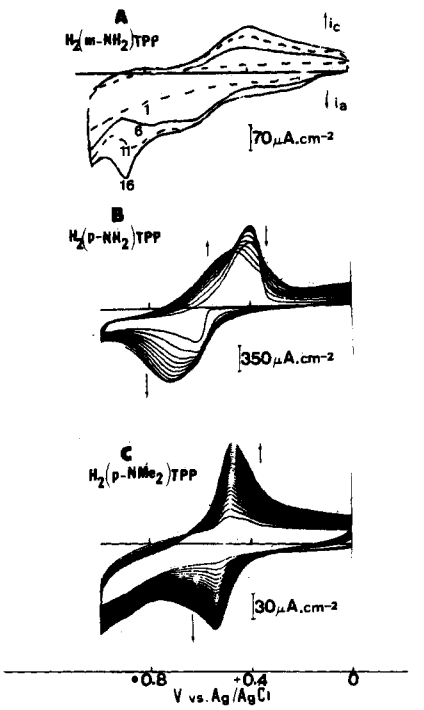

Figure 4. Cyclic voltammetric scans (200 mV/s) at a GC electrode in 0.1 M Bu_4NClO_4/CH_2Cl_2: (A) 1 mM H_2(*m*-NH_2)TPP (numbers below voltammograms are scan numbers); (B) 1 mM H_2(*p*-NH_2)TPP (recorded every second scan); (C) 1 mM H_2(*p*-NMe_2)TPP.

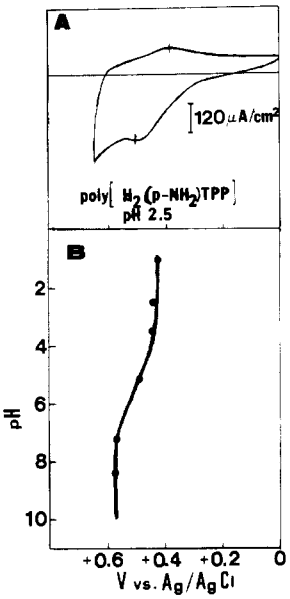

Figure 5. (A) Cyclic voltammogram for a poly-H_2(p-NH_2)TPP film (obtained as in Figure 4B) after being transferred to a 1 M NaCl solution containing 10^{-2} M phosphate buffer and adjusted to pH 2.5. (B) Plot of formal potential vs. pH for the poly-H_2(p-NH_2)TPP film shown in (A).

4). Electroreactivity in this potential range could reflect formation of either N-phenyl-p-phenylenediamine or o-benzidine moieties.[26] The anodic cyclic voltammetry of a poly-[H_2(p-NH_2)TPP] film in monomer-free aqueous solution (Figure 5A) shifts as a function of pH over pH 4–6 (Figure 5B) but shows no pH dependency in the pH ranges 0–4 and 6–9. Apparently the potential of the redox process of the coupled aminophenyl groups is influenced by an acid site that has $pK_a \approx 5$.

***p*-(*N*-Pyrrole)-Substituted Tetraphenylporphyrin.** The formation of α,α'-coupled polymers from the oxidation of pyrrole and variously N-substituted pyrroles is well-documented.[5g] Accordingly, a porphyrin-substituted pyrrole was anticipated to straightforwardly yield polymeric films upon oxidation, and this was indeed observed as shown in Figure 6. The initial potential scan in H_2(p-pyr)TPP solution produced a peak (Figure 6B) at about +1.0 V, about 300 mV more positive than the potential required for oxidation of 1-phenylpyrrole[27] (Figure 6A). Subsequent repetitive potential scanning revealed growth of a redox couple at $E^{\circ\prime}$ = +0.3 V, which probably represents a polypyrrolic reaction. We have no evidence for exceptional conductivity properties of these films, probably because of steric and cross-linking effects that prevent growth of long polypyrrole chains.

***p*-Hydroxy-Substituted Tetraphenylporphyrins.** The available redox chemistry for hydroxyphenylporphyrins shows their dual functionality: porphyrin and polyphenol.[28] The H_2(p-OH)TPP compound was insoluble in CH_2Cl_2 and CH_3CN, but the Ni^{II}(p-OH)TPP and Co^{III}(p-OH)TPP complexes could be oxidatively electropolymerized from CH_3CN as shown in Figure 7A. More positive potentials are required to electropolymerize the hydroxy compounds (about +1.4 V) than the amino- (about +1.1 V) and pyrrole-substituted porphyrins (about +1.2 V, Table III). Like the other Co(III) porphyrins, electropolymerized poly-Co(p-OH)TPP films (Figure 7B) do not show a clean Co(III) → Co(II) cyclic voltammetric wave in 0.1 M Et_4NClO_4/CH_3CN; that reaction is not initiated until potentials sufficient to generate a mediating Co(I) state are attained, whereupon a two-electron reduction occurs. The Co(II) → Co(III) reaction occurs in an ill-defined process at about +0.4 V. The reversible Co(II/I) reaction is most clearly observed by restricting the range of potential sweep (dashed line, Figure 7B).

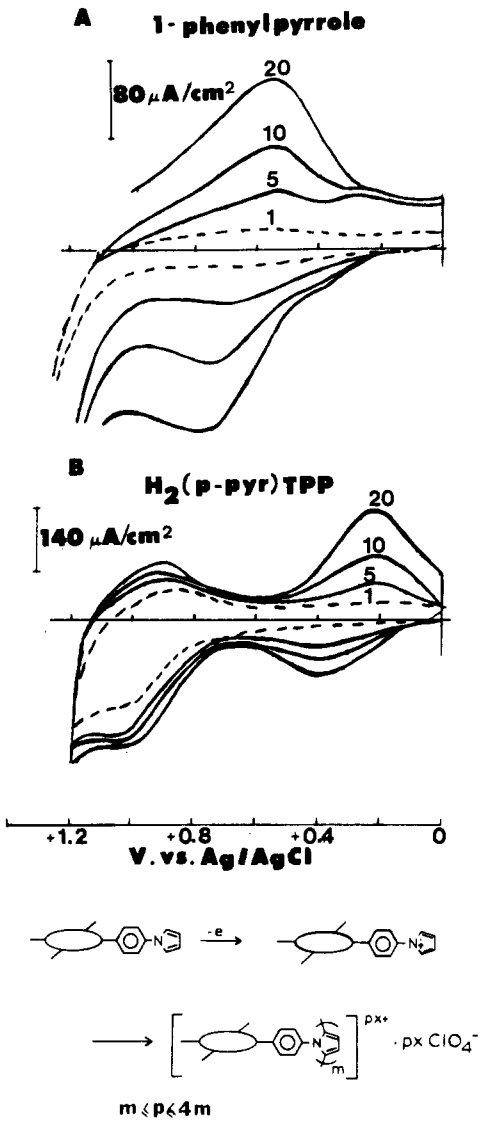

Figure 6. (A) Cyclic voltammetric scans (200 mV/s) at a GC electrode: (A) 1 mM 1-phenylpyrrole in 0.1 M Bu_4NClO_4/CH_2Cl_2; (B) 1 mM H_2(p-pyr)TPP in 0.1 M Bu_4NClO_4/CH_2Cl_2. Numbers above voltammograms are scan numbers.

Unexpectedly, films could also be formed from Co(p-OH)TPP solutions by reductive scanning around the potential of the Co(II/I) wave (Figure 7C). This behavior was not exhibited by Ni(p-OH)TPP or any of the other cobalt porphyrins. This phenomenon may somehow be associated with the hydroxy group acidity and the ability of the Co(I) state to form Co(III)–H species such as described by Spiro.[24b] Exactly how such chemistry subsequently leads to film formation is presently a subject of speculation. One clear feature of the reductively formed Co(p-OH)TPP films is, however, that they are more ordered, as is demonstrated, relative to the oxidatively formed film (E_{fwhm} = 220 mV in Figure 7B), by much sharper Co(II/I) voltammetry (E_{fwhm} = 120 mV in Figure 7D). The Co(II) → Co(III) wave is also better defined (Figure 7D).

The oxidatively formed films of the free-base porphyrins and metalloporphyrins listed in Table III are insoluble in a variety of common solvents such as Me_2SO, acetone, CH_2Cl_2, CH_3CN, DMF, and concentrated acids (HNO_3, H_2SO_4) and bases (NaOH). Solubility in DMF and aqueous acids was observed for poly-H_2(p-NH_2)TPP and poly-Ni(p-NH_2)TPP films grown at low oxidation potentials. While oxidatively formed Co(p-OH)TPP films were insoluble in all solvents tested, the reductively formed

(26) (a) Adams, R. N. *Electrochemistry at Solid Electrodes*; Marcel Dekker: New York, 1969; p 351. (b) Oyama, N.; Ohsaka, T.; Shimizu, T. *Anal. Chem.* **1985**, *57*, 1526.
(27) Salmon, M.; Carbajal, M. E.; Juarez, J. C.; Diaz, A.; Rock, M. C. *J. Electrochem. Soc.* **1984**, *131*, 1802.
(28) Evans, T. A.; Srivatsa, G. S.; Sawyer, D. T.; Traylor, T. G. *Inorg. Chem.* **1985**, *24*, 4733.

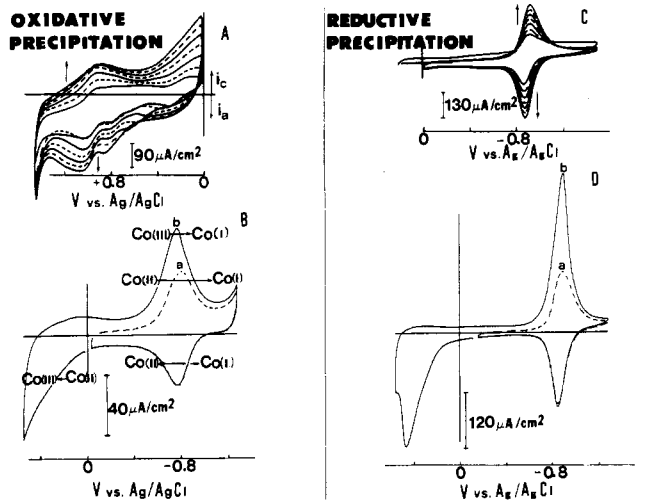

Figure 7. (A) Cyclic voltammetric scans (200 mV/s) in the range 0 → +1.4 V for 1 mM Co(*p*-OH)TPP in 0.1 M Et_4NClO_4/CH_3CN (recorded first and every fifth scan thereafter). (B) Cyclic voltammogram (50 mV/s) for a Pt/poly-Co(*p*-OH)TPP electrode with $\Gamma = 2.0 \times 10^{-9}$ mol/cm² formed as described in (A) and transferred to a Et_4NClO_4/CH_3CN solution. (C) Cyclic voltammetric scans (200 mV/s) in the range 0 → 1.5V for the same solution as in (A) (first and every fifth subsequent scan). (D) Cyclic voltammogram for a Pt/film electrode with $\Gamma = 4.2 \times 10^{-9}$ mol/cm² formed as described in (C). Dashed curves (a) are obtained for scans in the range 0 → −1.3V, and solid curves (b) are obtained for scans in the range +0.6 → −1.3V.

Table IV. Electroreduction of Dioxygen by Various Cobalt Porphyrin Films[a]

electropolymerized monomer	electrolyte[b]	$E^{\circ\prime}$, V vs. Ag/AgCl (without O_2)	$E_{p,c}$, V vs. Ag/AgCl (with O_2)	slope,[c] mA/[(V/s)$^{1/2}$ cm²]
Co(*o*-NH_2)TPP	H_2SO_4	+0.23, −0.08	+0.31	2.8
	NaOH	−0.16, −0.45	−0.25	3.1
Co(*m*-NH_2)TPP	H_2SO_4	+0.11	+0.06	1.3
	NaOH	−0.31	−0.34	2.1
Co(*p*-NH_2)TPP	H_2SO_4	+0.19	+0.13	1.5
Co(*p*-OH)TPP	H_2SO_4	+0.28[d]	+0.25[d]	2.2[d]
	NaOH	−0.20[e]	−0.27[e]	2.2[e]
Co(*p*-pyr)TPP	H_2SO_4	+0.02	+0.10	1.4
	NaOH	−0.30	−0.35	2.0

[a] Surface coverages ranged from 1.5×10^{-10} to 15×10^{-10} mol/cm². [b] 0.5 M H_2SO_4 or 1 M NaOH. [c] Slope of plot of cyclic voltammetric peak current divided by electrode area (i_p/A) vs. square root of scan rate ($v^{1/2}$). [d] For both oxidatively and reductively formed films. [e] For oxidatively formed films.

films could be dissolved in Me_2SO and in 3 M NaOH. Applying oxidative potential scanning to the reductively formed poly-Co(*p*-OH)TPP films, on the other hand, decreased their solubility in Me_2SO and base.

Electropolymerization in Aqueous Solutions. Oxidative electropolymerizations were observed for both aminoporphyrins (aqueous acid) and hydroxyporphyrins (aqueous base). Oxidative electropolymerization patterns, which commence at about +0.8 V, are compared in Figure 8 for Co(*o*-NH_2)TPP in 1 M methanesulfonic acid and 0.1 M Et_4NClO_4/CH_3CN. Waves for the Co(III/II) reaction can be observed in acid (Figure 8A) during electropolymerization but not in CH_3CN. Both films of Figure 8 exhibit a typical Co(II/I) wave in 0.1 M Et_4NClO_4/CH_3CN and a split Co(III/II) wave[14] in 0.5 M H_2SO_4 ($E^{\circ\prime}$ = +0.25 and −0.08 V) and in 1 M NaOH ($E^{\circ\prime}$ = −0.16 and −0.45 V). The poly-Co(*o*-NH_2)TPP film is unique, however, in exhibiting the double Co(III/II) wave; the other electropolymerizable cobalt porphyrins exhibit only *one* Co(III/II) peak in aqueous acid or base (Table IV).

Electropolymerization occurs in a very sharp wave at +0.1 V in aqueous base (1 M NaOH) for H_2(*p*-OH)TPP (when scanning potential between 0 and +0.5 V). As is often observed for polyphenoxy films,[4] the currents decrease upon continued electropolymerization, indicating passivation by formation of a nonconductive film.

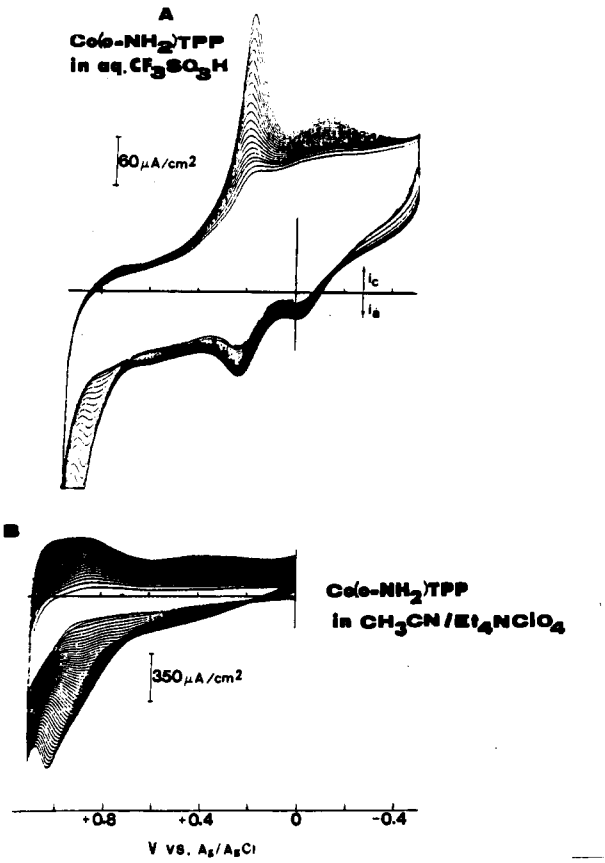

Figure 8. Cyclic voltammetric scans (200 mV/s) for 1 mM Co(*o*-NH_2)TPP in (A) 1 M CH_3SO_3H and (B) 0.1 M Et_4NClO_4/CH_3CN.

Film Structure and Spectroscopy. The general insolubility of the electropolymerized films hampers detailed structural investigations. The central evidences we have are as follows: (i) Electropolymerizations require the presence of substituents (amino, pyrrole, hydroxy) that are known in elementary aromatic form (aniline, 1-phenylpyrrole, phenol) to oxidatively electropolymerize, so that it is rational to expect similar types of coupling reactions. (ii) The electrochemical reduction potentials of the films are similar (Table III) to those of corresponding monomers, meaning that the porphyrinic structure is retained. (iii) Optical spectra of films deposited on SnO_2 electrodes closely resemble those of the dissolved monomers dissolved in CH_2Cl_2, as illustrated for monomeric Co(*p*-pyr)TPP and poly-Co(*p*-pyr)TPP (solid curves in Figure 2). A spectrum very similar (dashed line, Figure 2B) to that of electropolymerized poly-Co(*p*-pyr)TPP could furthermore be obtained by electropolymerizing free-base H_2(*p*-pyr)TPP and then inserting cobalt into the film (see Experimental Section). On the other hand, only one Soret band was observed for polymeric cobalt porphyrin films (Table I), at all surface coverages and in all solvent/electrolyte combinations used, which contrasts with the Soret splitting described above and interpreted as aggregation for the monomeric cobalt porphyrin solutions (Table I). It may be that splitting is present but is obscured because the Soret bands are broadened for the film spectra. (iv) The infrared spectroscopy of these films is difficult because of the small quantities involved, although Spiro et al.[15] have succeeded in obtaining considerable Raman evidence. We were able only to observe the IR spectrum of a poly-Co(*p*-pyr)TPP film (on SnO_2), which is compared (dashed curve) to that of Co(*p*-pyr)TPP in KBr (solid line) in Figure 9. The peaks at 3100, 1610–1505, and 725 cm^{-1} are characteristic of the various vibration modes of the C–H and C–C bonds of the aromatic nuclei;[29] those at 1350–1250 cm^{-1} arise from

(29) Dolphin, D.; Wick, A. In *Tabulation of Infrared Spectral Data*; Wiley-Interscience: New York, 1977.

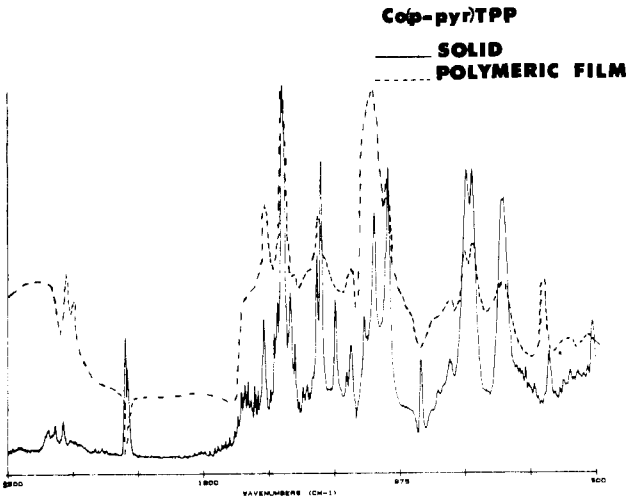

Figure 9. IR spectra for Co(*p*-pyr)TPP in KBr (solid line) and a poly-Co(*p*-pyr)TPP film on a SnO_2 electrode (dashed line).

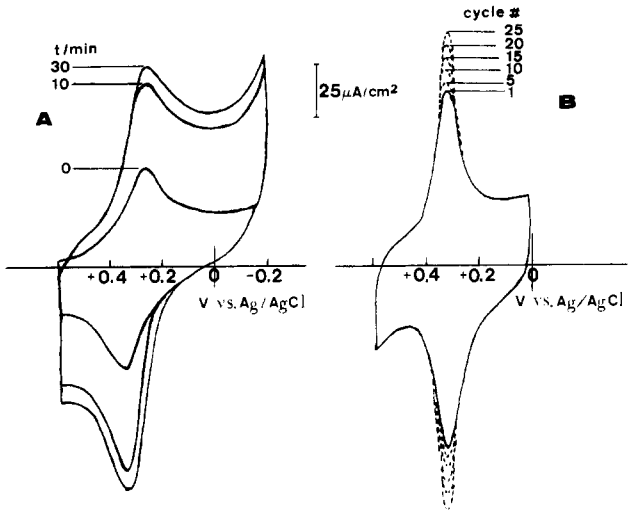

Figure 10. (A) Cyclic voltammograms (200 mV/s) for $Fe(CN)_6^{3-}/Fe(CN)_6^{4-}$ recorded continuously at a GC/poly-Co(*p*-pyr)TPP film electrode in a 0.1 M KCl solution containing 10^{-4} M $K_3Fe(CN)_6$. (B) Cyclic voltammograms (200 mV/s) obtained when the electrode used in (A) was washed with water and transferred to a 1 M KCl solution.

stretching vibrations of the C(phenyl)–N(pyrrole) bond, while those at about 1000 cm^{-1} can be assigned to N–H of the pyrrole groups in the center of the porphyrin molecule.[30] Peaks in the ≤700-cm^{-1} region are attributable to the ClO_4^- counteranion.[29]

Ion-Exchange Properties of the Films. The tactic of incorporating electroactive cations and anions into polyionic films on electrodes has been extensively employed to prepare electroactive films.[16,31] In the present case, such incorporation was used to probe the ionic charge state of the polymeric porphyrin films. Cyclic voltammograms in Figure 10A show that $Fe(CN)_6^{3-}$ is incorporated into a poly-Co(*p*-pyr)TPP film from aqueous 10^{-4} M $K_3Fe(CN)_6$/0.1 M KCl. The $Fe(CN)_6^{4-/3-}$ wave gradually increases in size with continued potential scanning. Interestingly, when the film was transferred after 30 min to pure supporting electrolyte, the wave *continued* to grow (Figure 10B). We interpret this behavior as reflecting a relatively low (slow) mobility of $Fe(CN)_6^{3-}$ ions in the film, e.g., Figure 10B represents slow diffusion of the $Fe(CN)_6^{3-}$ ions from the solution-exposed outermost layers to the innermost layers of the poly-Co(*p*-pyr)TPP film next to the electrode. Incorporation of $Fe(CN)_6^{3-}$ was also observed for poly-Co(*o*-NH_2)TPP and poly-Co(*o*-NMe_2)TPP films, but the effect in Figure 10B was not seen for these films. The general conclusion we draw from these results is that, at neutral aqueous pH values, the poly-Co(*p*-pyr)TPP, poly-Co(*o*-NH_2)TPP, and poly-Co(*o*-NMe_2)TPP films have a polycationic character in the range of potentials scanned in Figure 10. This conclusion is supported by observations that poly-Co(*o*-NH_2)TPP films form membrane barriers to cationic reactants like methylviologen.

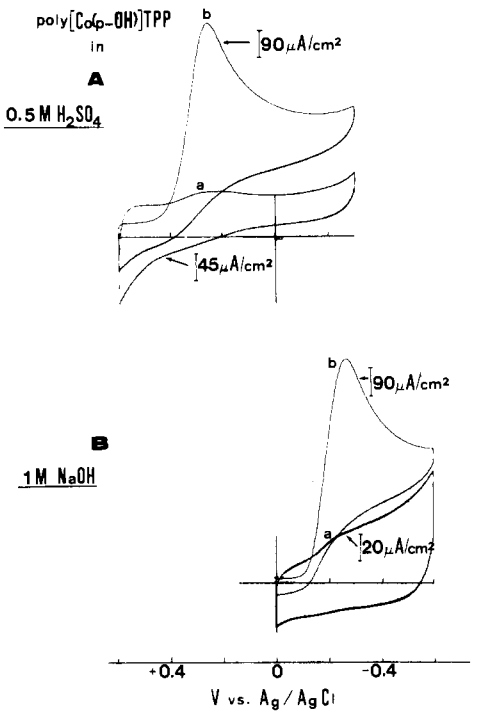

Figure 11. Cyclic voltammograms (100 mV/s) for a GC/poly-Co(*p*-OH)TPP film ($\Gamma = 1.3 \times 10^{-9}$ mol/cm^2) in (A) 0.5 M H_2SO_4 and (B) 1 M NaOH. Curves a and b are obtained in deaerated and O_2-saturated solutions, respectively.

In contrast, poly-Ni(*p*-OH)TPP films can be polyanionic (cation exchangers), since they incorporate $Ru(NH_3)_6^{3+}$ from aqueous 2×10^{-5} M $Ru(NH_3)_6^{3+}$/1 M NaCl/pH 8.3 phosphate buffer (10^{-2} M). The ionic incorporation was not stable, however; peaks for the $Ru(NH_3)_6^{3+/2+}$ couple ($E^{\circ\prime} = -0.2$ V) decreased to about 60% of their original height after being transferred to 1 M NaCl/pH 8.3 phosphate buffer solutions.

Catalytic Properties of the Films. Having shown[14] that poly-Co(*o*-NH_2)TPP films catalytically reduce O_2 to H_2O_2 or to water, depending on surface coverage and solution pH, we also tested the other electropolymerized cobalt porphyrin films for O_2 catalysis. Results comparing deaerated and O_2-saturated 0.5 M H_2SO_4 and 1 M NaOH are illustrated in Figure 11 for a poly-Co(*p*-OH)TPP film and are summarized in Table IV. We found that the poly-Co(*o*-NH_2)TPP films were unique in exhibiting a split Co(III/II) reduction wave[14] (Table IV); all of the other cobalt porphyrin films show only one wave. By the crude measure of the peak currents for the similarly shaped O_2 catalyzed waves, the poly-Co(*o*-NH_2)$_4$TPP film is also the best O_2 catalyst. The theoretical value of $i_p/Av^{1/2}$ for a four-electron reduction of O_2 is 3.2 mA/[cm^2(V/s)$^{1/2}$] for an O_2 concentration of 1.45×10^{-3} M (O_2-saturated solutions[32]) and diffusion coefficient[33] $D_{O_2} = 2.6 \times 10^{-5}$ cm^2/s. Table IV shows the slopes of i_p/A vs. $v^{1/2}$ plots for oxygen catalysis by the various films. poly-Co(*o*-NH_2)TPP films are the best catalysts as judged from both their more positive

(30) Alben, J. O. In *The Porphyrins*; Dolphin, D., Ed.; Academic: New York, 1978; Vol. III, pp 323–345.
(31) (a) Oyama, N.; Shimomura, T.; Shigehara, K.; Anson, F. C. *J. Electroanal. Chem. Interfacial Electrochem.* **1980**, *112*, 271. (b) Buttry, D. A.; Anson, F. C. *J. Am. Chem. Soc.* **1983**, *105*, 685. (c) Anson, F. C.; Ohsaka, T.; Saveant, J. M. *J. Am. Chem. Soc.* **1983**, *105*, 4883.
(32) Linke, W. F. *Solubilities of Inorganic and Metal Compounds*, 4th ed.; American Chemical Society: Washington, DC, 1965; Vol. II, p 1228.
(33) Kolthoff, I. M.; Miller, C. S. *J. Am. Chem. Soc.* **1941**, *63*, 1013.

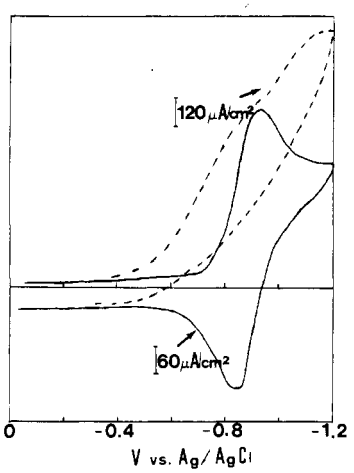

Figure 12. Cyclic voltammogram (200 mV/s) for a GC/poly-Co(*p*-NMe_2)TPP film ($\Gamma = 1.4 \times 10^{-9}$ mol/cm^2) in a CH_3CN + 0.1 M Et_4NClO_4 solution (solid curve) and for the same solution after addition of 2 volumes of H_2O (dashed curve).

potentials for O_2 reduction and larger slope. The slope for poly-Co(*o*-NH_2)TPP in 1 M NaOH is in fact very close to the four-electron value; we have confirmed by the rotating ring-disk technique[14] that this situation produces virtually no H_2O_2 product.

Assuming (as we have[14]) that the two waves for poly-Co(*o*-NH_2)TPP reflect monomeric and dimeric species in the film, then the lower activity of the other cobalt porphyrins may be connected to their lower dimerization constants, as found for Co(*p*-OH)TPP and Co(*p*-pyr)TPP solutions from absorbance spectroscopy (Table II).

Finally, Spiro et al.[24b] showed that Co(I) porphyrins placed in solutions and adsorbed or bound to GC electrodes[34] react rapidly with water. Figure 12 shows a test for water reduction using an electropolymerized poly-Co(*p*-NMe_2)TPP film (GC electrode). Co(II/I) voltammetry of the film in dry 0.1 M Et_4NClO_4/CH_3CN (solid curve) occurs at $E^{\circ\prime} = -0.92$ V, whereas upon addition of two volumes of water (dashed curve), an irreversible, split (ca. −0.68 and −1.01 V) wave, with greatly enhanced cathodic current and no reverse anodic wave, is observed. While it is reasonable to suppose that these waves represent H_2 evolution, they are not very stable (as Spiro[34] also experienced) and gradually decayed. No further studies were done. This instability is not characteristic of the polymeric porphyrin films in dry solvent, which in the potential window 0 to −1.5 V are very stable to repeated potential cycling.

Acknowledgment. This research was supported in part by a grant from the National Science Foundation.

(34) Kellet, R. M.; Spiro, T. G. *Inorg. Chem.* **1985**, *24*, 2378.

Contribution from the Department of Chemistry, University of Arizona, Tucson, Arizona 85721, and Chemistry Department, University of Manchester, Manchester M13 9PL, England

Syntheses, Structures, and Spectroscopic Properties of Six-Coordinate Mononuclear Oxo-Molybdenum(V) Complexes Stabilized by the Hydrotris(3,5-dimethyl-1-pyrazolyl)borate Ligand

W. E. Cleland, Jr.,[1a] Kerry M. Barnhart,[1a] Katsumoto Yamanouchi,[1a] David Collison,[1b] F. E. Mabbs,[1b] R. B. Ortega,[1a] and John H. Enemark*[1a]

Received September 5, 1986

A series of 19 mononuclear oxomolybdenum(V) compounds of the general formula LMoOXY (L = hydrotris(3,5-dimethyl-1-pyrazolyl)borate; (X,Y) = Cl^-, NCS^-, N_3^-, OR^-, SR^-, and the dianions of ethylene glycol, mercaptoethanol, dimercaptoethane, catechol, *o*-mercaptophenol, *o*-aminophenol, *o*-aminobenzenethiol, and toluenedithiol) have been prepared and characterized by electron paramagnetic resonance spectroscopy (EPR), cyclic voltammetry, UV–visible spectroscopy, and mass spectrometry. The $LMoO(SR)_2$ complexes possess the cis sulfur ligands proposed for the molybdenum cofactor. The structure of $LMoO(SPh)_2$ was determined by X-ray crystallography: space group $P2_1/c$, $Z = 4$, $a = 13.079$ (6) Å, $b = 14.438$ (7) Å, $c = 15.836$ (9) Å, $\beta = 104.73$ (4)°. The molecule adopts the expected *fac* six-coordinate stereochemistry with cis thiolate groups. The average Mo–S distance is 2.382 (2) Å, and the average Mo–O distance is 1.676 (4) Å. The Mo–N distances range from 2.164 (5) to 2.357 (5) Å. The isotropic $\langle g \rangle$ and $\langle A \rangle$(^{95,97}Mo) values show an inverse correlation and cluster according to the nature of the donor atoms. Sulfur donor atoms lead to large $\langle g \rangle$ and small $\langle A \rangle$ values. The anisotropies of the *g* values for $LMoO(OR)_2$ and $LMoO(SR)_2$ complexes show marked differences between monodentate and chelated ligands. All LMoOXY complexes undergo reversible one-electron reductions. The reduction potentials span a range of 1.3 V depending upon the nature of X and Y; $LMoO(NCS)_2$ is most easily reduced, and $LMoO(OCH_2CH_2O)$ is the most difficult to reduce. Complexes become easier to reduce as alkoxide groups are replaced by thiolate groups.

Introduction

Molybdenum is an essential trace element which is found in enzymes such as xanthine oxidase, sulfite oxidase, and nitrate reductase.[2,3] The chemical reactions catalyzed by these enzymes all involve a change in the number of oxygen atoms in the substrate, and there is strong evidence that these enzymes possess a common molybdenum cofactor (I).[4,5] EXAFS studies support

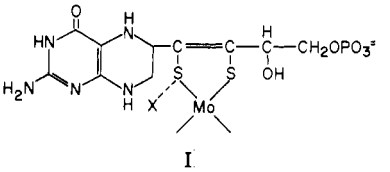

I

a mononuclear molybdenum center with at least two RS^- ligands bound to the molybdenum atom.[6,7]

An overall chemical reaction cycle for oxo–molybdenum centers of such enzymes involving Mo(IV), Mo(V), and Mo(VI) is shown

(1) (a) University of Arizona. (b) University of Manchester.
(2) Spence, J. T. *Coord. Chem. Rev.* **1983**, *48*, 59–82.
(3) *Molybdenum and Molybdenum-Containing Enzymes*; Coughlan, M. P., Ed.; Pergamon: New York, 1980.
(4) Johnson, J. L.; Rajogopalan, K. V. *Proc. Natl. Acad. Sci. U.S.A.* **1982**, *79*, 6856–6860.
(5) Cramer, S. P.; Stiefel, E. I. In *Molybdenum Enzymes*; Spiro, T. G., Ed.; Wiley: New York, 1985; Chapter 8, pp 411–441.
(6) (a) Cramer, S. P.; Wahl, R.; Rajagopalan, K. V. *J. Am. Chem. Soc.* **1980**, *103*, 7721–7727. (b) Bordas, J.; Bray, R. C.; Garner, C. D.; Gutteridge, S.; Hasnain, S. S. *Biochem. J.* **1980**, *191*, 499–508.
(7) Cramer, S. P. *Adv. Inorg. Bioinorg. Mech.* **1983**, *2*, 259–316.

0020-1669/87/1326-1017$01.50/0